Research Article

Analysis of cosmic ray, solar wind energies, components of Earth's magnetic field, and ionospheric total electron content during solar superstorm of November 18–22, 2003

Binod Adhikari[1,2] · **Bidur Kaphle**[1] · **Niraj Adhikari**[1] · **Sanam Limbu**[1] · **Aashish Sunar**[1] · **Roshan Kumar Mishra**[1] · **Sarala Adhikari**[3]

Abstract

This paper studies the impacts of interplanetary coronal mass ejections (ICMEs) preceding storm (November 18–22, 2003) on several space weather components. The comprehensive study of different parameters such as solar wind speed, density, plasma temperature, plasma pressure, auroral electrojet, SYM-H, energy transfer, components of Earth's magnetic field, total electron content, and cosmic ray received by Earth during the ICME storm has been studied, which accounts for the more precise knowledge of the storm from different dimensions. The solar storm of November 2003 had SYM-H value of −472 nT. During the main phase of the storm, the velocity of solar wind reached approximately to 500 km/s, and plasma pressure cumulated to around 20 nPa. The total energy dissipated during the storm in the magnetosphere has been converted in the form of ring current, joule heating, and auroral precipitation. The joule heating leads to modification in thermospheric contents and traveling atmospheric contents that result in further modification of the density, composition, circulation, and dynamics of ionosphere–thermosphere system. This phenomena further result in the escalation and slumping of TEC. We found out the decrease in rate of cosmic ray received by the Earth during the main phase of the storm, which lead to our conclusion that there exists inverse relation between strength of solar storm and amount of cosmic ray fluxes received by the Earth. In addition, the study made on the change in TEC and SYM-H during the event hinted us toward the possible changes in the space weather caused by the solar superstorm of November 18–22, 2003.

Keywords Geomagnetic storms · ICMEs · Solar cycle · TEC · Energy of Earth · Earth's magnetic field · Cosmic ray

1 Introduction

Coronal mass ejections (CMEs) are the activity of the solar corona in which a huge mass of plasma gets ejected. Plasma moves radially outward due to the combined effect of the radial outward motion of the plasma and the rotation of the sun. This also causes the magnetic lines to become spiral in shape. ICMEs contain a bunch of plasma, ions, electrons, and other solar particles along with a large amount of energy [22]. The complex group of CMEs, sometimes with their leading shock waves, has been called ICMEs amid their helispherical propagation [31]. The north–south component of southward directed IMF-Bz plays a major role in determining the amount of energy to be transferred to geo-magnetosphere. When IMF has a large magnitude (≥ 10 nT) and a large southward component, the amount of transferred energy becomes large. The transferred energy gets low when the IMF is directed preliminary northward [16]. According to Tsurutani et al. [51], the extreme volume of southward directed IMF Bz are the primary causes of great magnetic storms rather than the solar wind. There are several forms for dissipation of

✉ Binod Adhikari, binod.adhi@gmail.com | [1]Department of Physics, St.Xavier's College, Maitighar, Kathmandu, Nepal. [2]Department of Physics, Patan Multiple Campus, Tribhuvan University, Kathmandu, Nepal. [3]Department of Physics, Tri-Chandra Multiple Campus, Tribhuvan University, Kathmandu, Nepal.

SN Applied Sciences (2019) 1:453 | https://doi.org/10.1007/s42452-019-0474-8

Received: 2 January 2019 / Accepted: 9 April 2019 / Published online: 13 April 2019

the energy in the magnetosphere; they are ring current (U_r), Joule heating (U_j), and Auroral precipitation (U_a) [4].

Ionosphere is the layer of the Earth's atmosphere that is ionized by solar and cosmic radiation. It lies above 75 to 1000 km above the Earth surface. The energy and energetic particles deposited in the polar upper atmosphere are effectively increased and drive notable changes in the compositions, temperature, circulation, and electric fields during an ICME event. So noteworthy disturbances are induced in total electron content (TEC) [8, 14, 33, 36, 38]. TEC is used to measure the ionospheric condition. As mentioned in Fagundes et al. [18], the strong positive ionospheric effect is observed during the main phase and the strong negative ionospheric effect is seen during the recovery phase. The ionospheric layers experience both increase and decrease in electron concentration relative to a background level and make up positive and negative phases, respectively [14]. One of the significant features of the positive phases is that sometimes they are observed even before the arrival of CMEs.

Moreover, the solar storms have huge impact on the rate of cosmic rays received by the Earth [5]. In addition, the ionization, which increases with geomagnetic latitude and decreasing solar activity [52], produced by the cosmic rays entering into the Earth's atmosphere results in disturbances observed mainly in electrical conductivity, global electric circuit and has huge impact on space weather phenomena [42].

Here in this paper, we have studied and discussed the impacts of the halo CME of October 18 to 22, 2003, on Earth's climate as a whole from ranging from solar wind to galactic cosmic rays. In this paper, Sect. 1 discusses introduction, Sect. 2 contains dataset, Sect. 3 contains results and discussion, Sect. 4 is about conclusion.

2 Dataset

In this paper, we have studied the effects of the geomagnetic storm of Nov 20, 2003, on cosmic ray, solar wind energies, components of Earth's magnetic field, and ionospheric total electron content. The necessary data for solar wind parameters and sunspot study were taken from Omni Web Data Explorer. https://omniweb.gsfc.nasa.gov/form/omni_min.html. The data for components of Earth's magnetic field and galactic cosmic ray data were taken from http://www.intermagnet.org/ and http://neutronm.bartol.udel.edu/~pyle/bri_table.html. The ionospheric total electron content was downloaded from ftp://cddis.gsfc.nasa.gov/pub/gps/data. The data for solar wind energy (*U*sw), ring current (*U*r), joule heating (*U*j), and auroral precipitation (*U*a) were calculated manually.

Table 1 The list of neutron monitor stations, their coordinates, and their cut-off rigidities

Stations	Coordinates
South Pole, Antarctica	90 S
McMurdo, Antarctica	77.9S, 166.6E
Thule, Greenland	76.5N, 68.7W
Newark, Delaware	39.7N, 75.7W
Swarthmore, Pennsylvania	39.9N, 75.4W

Table 2 The list of magnetometer stations and their coordinates

Stations	Coordinates
Boulder	40.02°N
Eyrewell	43.42°S
Scott base	77.85°S
Thule	77.47°N

The list of cosmic ray stations and their coordinates are as follows: (Tables 1, 2).

3 Results and discussions

Section 3.1 discusses the impacts of halo CME of November 20, 2003, on solar wind parameters, IMF-Bz, and geomagnetic indices. Similarly, Sect. 3.2 discusses the sunspot cycle from 1996 to 2008. Section 3.3 discusses the solar wind energy (*U*sw), ring current (*U*r), joule heating (*U*j), and auroral precipitation (*U*a); Section 3.4 observed the impacts of solar storm on components of Earth magnetic field; and Sects. 3.5 and 3.6 discuss the variation on total electron content and cosmic rays, respectively.

3.1 Solar wind parameters, IMF-Bz and geomagnetic indices (AE and SYM-H) during November 19–22, 2003

The solar superstorm that occurred on November 20, 2003, was the result of the CME [23]. Its magnetic cloud was found to have a high axial magnetic field (approx. 56 nT) and high inclination (~ 73.4°) to the ecliptic plane. Thus, it had a strong southward component, making it geoeffective [21]. The CME reached to strike the magnetosphere at around 8 a.m on the 20 November. In Fig. 1, we can see that the ICME had initial, main, and recovery phases. The lagging of SYM-H behind other parameter tells that the geomagnetic storm causes a disturbance in *H* component after a certain period of time, not simultaneously [53]. In the figure, the SYM-H index has not recovered completely even until 22 November. IMF-Bz differs slightly from SYM-H due to its small rise before the endpoints of initial

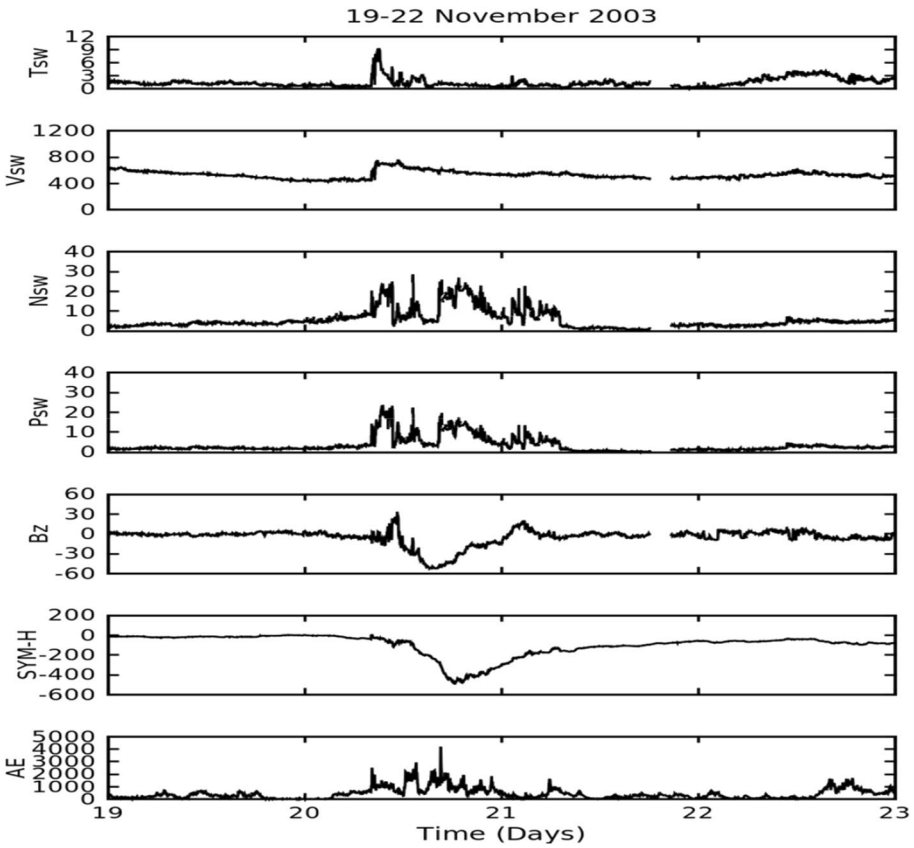

Fig. 1 Graph showing temperature (T_{sw}), velocity (V_{sw}), density (N_{sw}), proton plasma pressure (P_{sw}), IMF-Bz (nT), SYM-H (nT), and AE (nT) during the ICME storm of November 19 to 22, 2003. Data downloaded from Omni Web Data Explorer, https://omniweb.gsfc.nasa.gov/form/omni_min.html

and recovery phase. The variation of IMF-Bz differs from SYM-H because of its less dependence on other factors like axial orientation and speed of magnetic cloud [23]. The main purpose of AE (Auroral Electrojet) index is to measure the global auroral zone magnetic activity produced by enhanced ionospheric currents, and we know that the AE is the difference of amplitude upper (AU) and amplitude lower (AL) AE = AU – AL, where AU is the eastward electrojet current densities and AL is the westward electrojet current densities [1–3]. The AE value of the storm was almost negligible before the storm time. After the storm on 20 November, it reached to the maximum value of approximately 4000 nT at midday of 20 November and eventually recovered by the early morning of 21 November.

We can also see that in this storm the average value of solar wind was approximately 450 km/s before the initial phase of solar storm, and it later attained the maximum value of around 580 km/s at around 8 a.m. The solar wind speed reached a maximum of about 700 km/s before noon and then gradually returned to the normal value. Also, the plasma temperature (*T*sw) showed a steep rise in the initial phase and attained the mean value in a short period of time. The temperature was constantly fluctuating but the fluctuation was relatively smaller. In the graph, we see the proton density fluctuates largely in comparison with the other parameters. The value of Nsw rose constantly from 08:00 UT on 20 November to reach the peak value of 30 cm^{-3} at around 12:00 a.m. and maintained around the value till decreasing at 06:00 UT on 21 November. Here, we can observe the variation of flow pressure matching closely to the variation of proton density.

3.2 The 23 sunspot cycle (1996 to 2008)

The period between 1996 and 2008, during which the sunspot number (SSN) increases and then decreases gradually, is considered solar cycle 23. In Fig. 2, we can see that SSN increased from 1996 to 2000 and then decreased from 2000 to 2001. In 2001, we can see a sharp rise in SSN. However, from that point, it decreases steadily until 2008. In February 2001, NASA reported the flipping of the Sun's

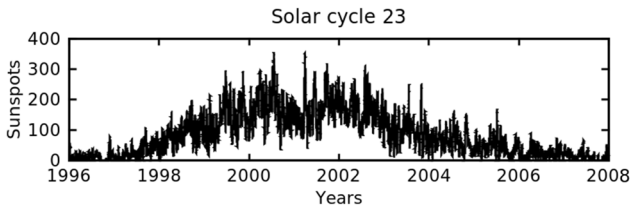

Fig. 2 The sunspot number in solar cycle 23 (1996 to 2008). Data downloaded from Omni Web Data Explorer, https://omniweb.gsfc.nasa.gov/form/omni_min.html

magnetic field, marking the peak of solar cycle 23 [25]. As solar cycles are asymmetric with respect to their maxima [26]—the rise to maxima is quicker than the decline to minimal and the rise time is shorter for larger amplitude cycle—solar cycle 23 had an increase in activity from 1996 to 2001 and then decrease until 2008. And although solar cycle has larger geomagnetic storms in the ascending phase, more storms occur during the descending phase [24]. Gonzalez et al. [20] claimed that there are often two leading peaks in a solar cycle, one in the ascending phase and the other in the descending phase. The average separation of the peaks from solar maximum is about 8 months for the first one and about 25 months for the second one [40]. In Fig. 2, the first peak is in 2000 and the second peak is in 2003. Siingh et al. [43] and Raizada et al. [39] concluded that the occurrence of intense geomagnetic storms is strongly correlated with SSN, but no significant correlation between the maximum and minimum phases of solar cycle and yearly occurrence of storms has been found. Solar cycle 23 experienced maximum number of geomagnetic storms in 2002, and the largest geomagnetic storm on November 20, 2003 [40]. It was also seen that phases of halo CMEs and solar cycle are not exactly the same. However, yearly occurrences of halo CMEs were followed by that of geomagnetic storms, thus making Halo CMEs responsible for the occurrence rate of GMSs during the solar cycle 23. It is evident that the solar super storm of 2003 was not expected. On the basis of previous works, it was claiming that the occurrence of super storms do not follow any particular trend, but can occur anytime in a solar cycle.

3.3 Solar wind energy (*Usw*), Ring current (*Ur*), Joule heating (*Uj*), and Auroral precipitation (*Ua*)

Figure 3 discusses the variation on ring current (*Ur*), joule heating of magnetosphere (*Uj*), and auroral precipitation (*Ua*) observed during the solar superstorm of 18–November 22, 2003. In fact, the ring current injection (*Ur*), joule heating of the magnetosphere (*Uj*), and auroral precipitation (*Ua*) are the major forms of dissipation of the energy in the magnetosphere [4, 15], so their study can give us information regarding the energy variations observed during the solar condition. At around 08:00 UT on 20 November, we observe a huge increment in energy content of the ionosphere. During the period, the energy increases to 1×10^{15} W and remains around the value till 08:00 UT of 21 November. The ring current injection (*Ur*) value increases with the storm and reaches to approximately 1.75×10^{13} W and then continues fluctuating till 08:00 UT 21 November. The value of *Uj* starts fluctuating in the range of 1×10^{12} W to ambient value by the start of storm on 20 November to its end on 21 November. The value of *Ua* fluctuates slightly and remains in the range of ambient value to 2×10^{11} W during the storm period. Moreover, the ring current injection (*Ur*) has varied slightly over the period from 18 to 22 November. Though the initial value around is 1×10^{15} W, the value of *Ur* rises gradually to 3×10^{11} W on midday of 20 November and gradually decreases to its normal position. In the graph, we can also see the energy at ring current (*Ur*) started to fluctuate since from 09:00 UT of 20 November and continues to vary till around 07:00 UT of

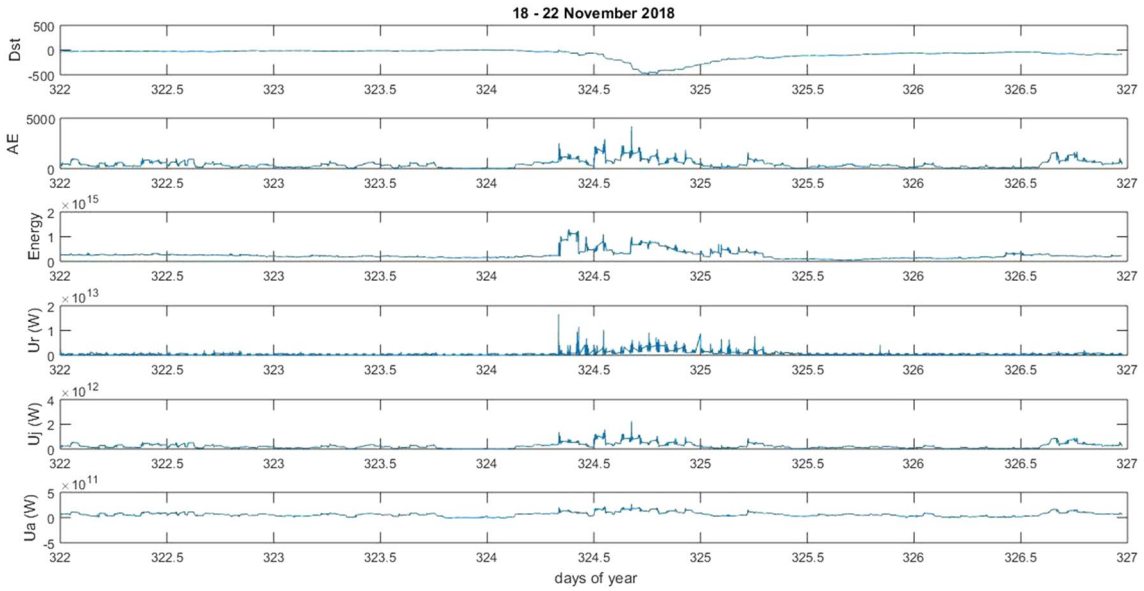

Fig. 3 Graph showing Dst (nT), AE, ring current (U_r) (W), joule heating (U_j) (W), and auroral precipitation (U_a) (W) of an ICME event November 18–20, 2003. Data were calculated manually

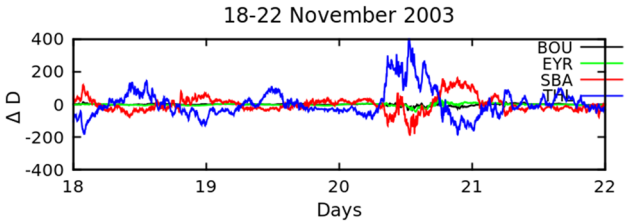

Fig. 4 Fluctuation of *D* component of Earth's magnetic field (nT) during 18–22 November 2003 of Boulder, Eyrewell, Scott Base and Thule. Data downloaded from http://www.intermagnet.org/

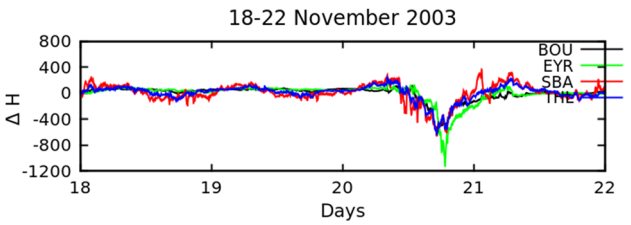

Fig. 5 Fluctuation of *H* component of Earth's magnetic field (nT) during 18–22 November 2003 of Boulder, Eyrewell, Scott Base and Thule. Data downloaded from http://www.intermagnet.org/

21 November. We get to study that the energy in the ring current reached a maximum of 1.5×10^{13} W during the first hour, but it couldn't maintain the position for so long and follow back to ambient value. The way of increasing and decreasing continued until the storm came to ease on 21 November (Figs. 4, 5, 6).

The graph also showed that the Dst lags behind the actual time of interaction between solar wind with the Earth's magnetic field. In our event, the recovery phase of ICME is gradual because Dst required almost one day to recover approximately 80% of its actual stage, whereas it had only taken a half day to reach its lowest point from the normal stage. The rate of decrement of *Ur*, *Uj*, *Ua*, and AE is also slow. *Uj*, *Ua*, and AE have also shown some slight increase before and after an ICME event, whereas Dst and ring current have fluctuated only in ICME event. This study tells us that the Dst and *Ur* are the more precise parameters for the study of an ICME rather than *Ua*, *Uj*, and AE. We have also observed that the ring current (*Ur*), joule heating (*Uj*), and auroral precipitation (*Ua*) are in the range of 10^9–10^{12} W, whereas the total energy of wind has been in the range of 1×10^{15}–10^{15} W. Mac-Mahon and Gonzalez [41] calculated that 1% to 4% of the energy available in the solar wind is transferred to the magnetosphere during the main phase of the geomagnetic storms, and in the average, about 25% to 40% of transferred energy is injected into ring current. In our study, we calculated the total energy of ICME to be 1.3×10^{15} W, so ultimately its

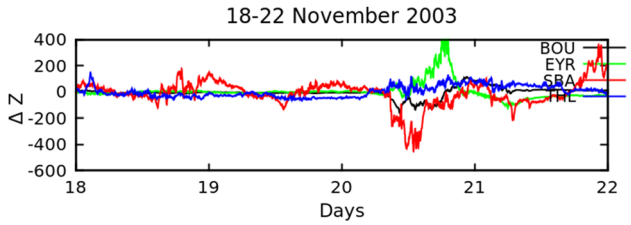

Fig. 6 Fluctuation of *Z* component of Earth's magnetic field (nT) during 18–22 November 2003 of Boulder, Eyrewell, Scott Base and Thule. Data downloaded from http://www.intermagnet.org/

ring current should have been between 3.25×10^{12} and 2.08×10^{13} W, but ring current calculated by us is only 1.4083×10^{12} W which is very less than compared to Mac-Mohan and Gonzalez's study.

3.4 Effect on *D*, *H*, and *Z* components of Earth's magnetic field

In this section, we analyze the variation of the solar storm of November 20, 2003, on *D*, *Y*, and *Z* component of Earth's magnetic field based on four different latitude stations of Boulder, Eyrewell, Scott Base, and Thule. The fluctuation of *D* component at Boulder and Eyrewell is negligible during whole observation period. In Scott Base, the solar variation decreases to -200 nT during the initial phase and increases to approximately 150 nT during the main phase and remains there for approximately 6 h. In case of Thule, the variation is completely opposite to Scott Base where the *D* component starts to increase since around 10:00 UT and reaches to approximately 350 nT. Maintaining itself around the range of 350 nT to 400 nT till 21:00 UT, it decreases back to 0 nT. Here again, the value of *D* component decreases to − 200 nT at around 22:00 UT on 20 November. The *H* component shows similar variation in all four stations. In *Z* component, the variations in four stations vary greatly. Boulder and Thule maintain to approximately 0 nT during the storm while Scott Base and Eyrewell maintain completely opposite graph. *Z* component of Eyrewell increases to 400 nT at around 21:00 UT and returns back to equilibrium while the *Z* components of Scott Base decreases to − 400 nT at around 13:00 UT. On the basis of variation of magnetic components of Earth, we can even calculate the strength of solar storm. The magnetic field produced by the current of solar energetic particles (SEPs) is opposite to the Earth's magnetic field and leads to a decrease in components of Earth's magnetic field. These SEPs are also the major component of the ring current system [12]. Thus, the decrease in the components of Earth's magnetic field, *D*, *H*, and *Z* was actually the effect of magnetic filed produced by current of SEPs and the formation of ring current [13].

Solar storm creates the magnetic disturbance in various components of the Earth magnetic field. The amount of variation in the Earth's component of the magnetic field varies on the basis of the strength of storm. We noticed similar variation in all components of Earth's magnetic field during the solar super storm of 2003. Ring current is a toroidal shaped current that flows westward around the Earth at the distance 4 to 9 R_E which is formed by the movement of energetic particle to the inner side of the Earth's magnetosphere. [13]. The publications of Chapman and Ferraro in the early 1930s suggested a transient stream of outflowing solar ions and electrons responsible for terrestrial magnetic storms; once the solar stream had reached the Earth, charged particles would leak into the magnetosphere and drift around the Earth and create a current whose field would oppose the main geomagnetic field [10, 11]. The only thing that has changed in this theory is transient stream changing to solar wind [35]. The magnetic field produced by this current is opposite to the Earth's magnetic field and so an earthly observer would observe a decrease in magnetic field in this area. Ions in the range 10–200 keV are responsible for majority of the ring current energy content [12]. The components of Earth's magnetic field, *D*, *H,* and *Z* as a result of ring current decrease by a considerable amount during the solar storm. Here the variation in *D* component, *H* component, and *Z* component of Earth's magnetic field during the lower end of 20 November marks the beginning of solar storm, and it continues till the end of storm.

3.5 A variation on total electron content

During the geomagnetic storm, in the upper atmosphere at higher altitude, the exalted amount of energy and the momentum gets heated due to Joule heating and fattens bestowing equatorward surges modification in thermospheric contents and traveling atmospheric disturbances [34, 37]. This results in the modification of the density, composition, circulation, and dynamics of ionosphere–thermosphere system, which is the root of escalating and slumping in total electron content(TEC) and electron plasma densities termed as positive and negative [33, 36]. The major component for the evolution of the positive ionospheric storm phase is prompt penetration electric fields, whereas the negative ionospheric storm phase emerges in the midlatitude region due to the overall effects of the equatorward shift of midlatitude density trough, the disturbance dynamo electric fields and compression of plasmapause in equatorial region along with the changes in chemical configuration [34]. During recovery phase, the vigorous negative ionospheric storm phase is perceived in both TEC and ionosonde observations indicating a robust hemispherical asymmetry [34]. Due to this reason, the total electron content is also regarded as the potent technique to study ionospheric storm. In fact, total electron content (TEC) is imperative factor of the ionosphere, which provides the idea regarding the navigation and the satellite-based communication.

In this work, we studied the variation of TEC from four stations Braz, Coco, Guug, and Glps to see the effect of the ICME on TEC on the basis of the local time of stations' locations. We observed the TEC graph separately by converting its time format into local time which was initially in Universal Time (UT), where Coco's local time (LT) = UT + 8 h, Guug LT = UT − 10 h, Braz LT = UT − 3 h, and Glps LT = UT − 6 h. By our observation of TEC on the local time of stations, we found that TEC graph was first disturbed in Guug (1:00 a.m.) on November 21. Then, it was subsequently followed by Braz and Coco. But Glps did not show any substantial change in its TEC, except a sudden increment during its decreasing time for a very short period. In addition, the TEC disturbance by the ICME in Guug and Braz lasted only for a period of 24 h, and they returned to their initial state afterward, but it continued for a long time in case of Coco. In addition, the TEC in Glps increased beyond the level of 100 toward the end of the ICME, which was the only instance among the four stations during the ICME. This indicates that the ICME from November 18 to 22, 2003, was followed by strong geomagnetic storms along with the support of long depression in TEC graph of Coco at the end of the ICME. The results show that the TEC from various stations of different latitudes have their own pattern as per the time of the day, which supports Mendillo and Klobuchar [32] approach of creating average TEC patterns as a function of latitude and local time that describe each day after the solar storm, significantly limiting their capacity to resolve the storm time evolution of features to once per 24 h. Immel and Mannucci [28] suspected that, on average, more significant storm occurs near the time of the afternoon/cusp TEC peak (18 to 24 UT), and this work clearly relates to TEC being in its maxima phase from 18 to 24 UT at Braz, Gipps, and Guug, but not at Coco. We also observed that the increment and decrement of TEC exhibits wave like feature which was also studied by Fagundes et al. [18].

3.6 Effect on galactic cosmic rays (GCR)

Cosmic rays entering into the Earth's atmosphere produce ionization which increases with the increasing geomagnetic latitude and decreasing solar activity [52]. This change in ionization often results in disturbance in electrical conductivity, global electric circuit, nucleation rates in cloud lightning discharges, space weather phenomena, etc. [5, 42–47, 49, 50]. This causes us to study the effect of cosmic ray in an urgent manner. We have studied the

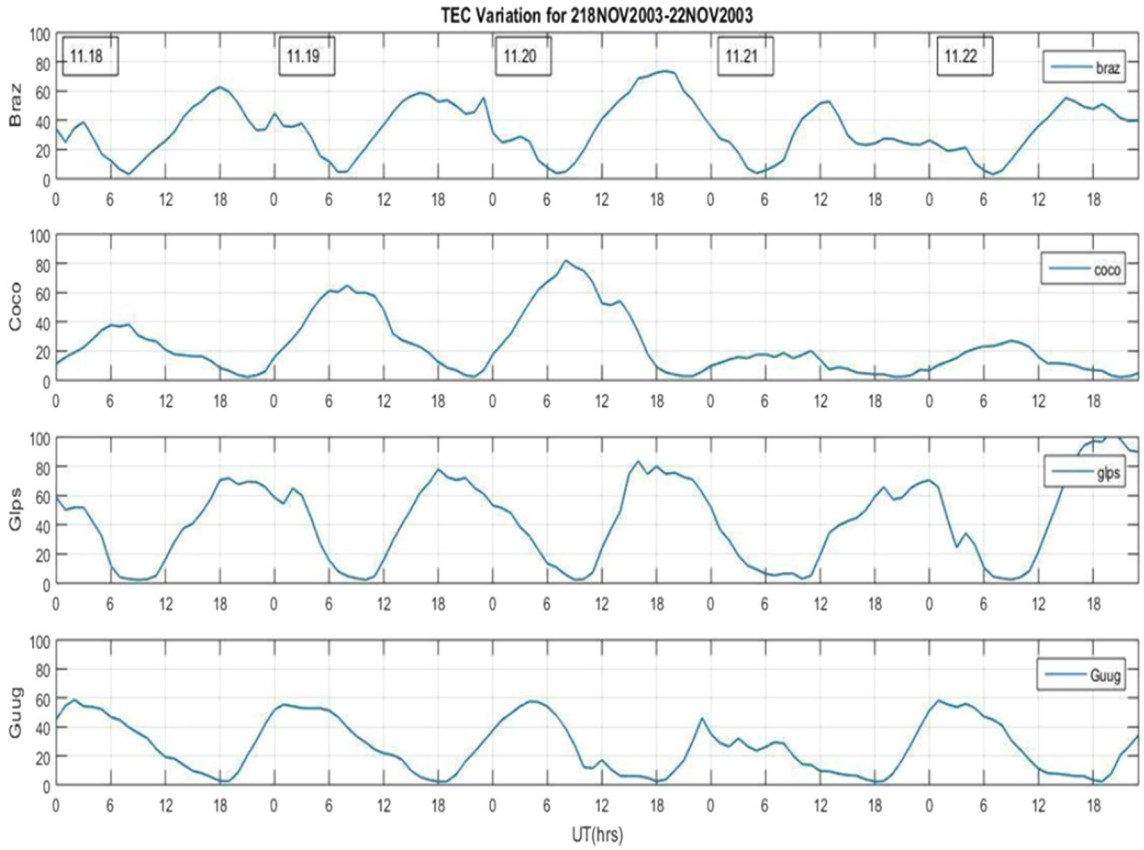

Fig. 7 TEC Variations (electrons/m^2) in four stations 1. Braz 2. Coco 3. Gips 4. Guug during an ICME event November 18–22, 2003. Data downloaded from ftp://cddis.gsfc.nasa.gov/pub/gps/data

data from four stations, which are McMurdo, Swarthmore, Thule, and South Pole. The geomagnetic cutoff rigidity of McMurdo, South Pole, and Thule station is close to zero, whereas the cutoff of Swarthmore is 1.92 GV.

The galactic cosmic ray received by McMurdo was slightly inconsistent at the start of 20 November, but it steeply rose by approximately 3.5% at around 09:00 UT. For Swarthmore, the amount of variation is a bit low and also the rate of change looks somewhat different which can be observed in Fig. 7. South Pole has the same nature of increasing on 20 November to decreasing continuously as of McMurdo. But Thule is of different nature than that of McMurdo and South Pole but resembles to that of Swarthmore. The rate of cosmic ray received by Swarthmore station is often increasing irrespective to other stations. It is constantly rising from 18 to 20 November till it starts decreasing. However, the rate of decrease is very less in comparison with as observed in other stations and the cosmic ray receiving rate is sometimes increasing also. Coronal mass ejections (CMEs) create very huge disturbances in the solar wind which mostly reaches the near-Earth space inside the generally high-speed plasma streams [48]. According to Kudela, [29] the magnetic field of the sun and Earth has a significant role in regulating the arrival of GCRs to the atmosphere. Forbush [19] and Hess and Demmelmair [27] were the first persons to notice the short-term depressions in GCRs, and hence, they termed it as "Forbush decreases" (FD). It was later noticed that the larger and faster CMEs [6, 7], CMEs with larger apparent width [6, 30] and CMEs with greater mass [6] had larger FD. Similarly Dumbovic et al. [17] grouped FD magnitudes [FD] into four different levels of GCR effectiveness: He categorized with FD < 1% as not GCR effective, whereas between 1 and 3% as moderately GCR effective, between 3 and 6% as strongly GCR effective, and those above 6% as intensively GCR effective. The cosmic ray received by the Earth during halo CME of 18 to 20 November is less than receiving rate in normal time. Hence we can conclude that the FD was strongly GCR effective. For more, GCRs play very important role in the ionization of environment [2, 3, 9] and have several other impacts in our surrounding. Since the cosmic rays received by the Earth decreased during 18 to 22 November, we can infer that the surrounding was less impacted by the cosmic rays during that period (Fig. 8).

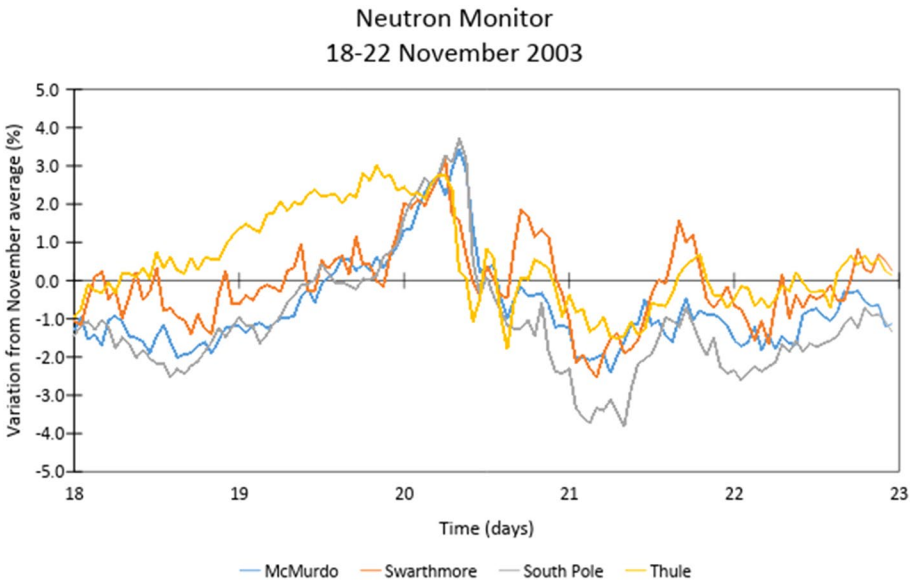

Fig. 8 Graph showing variation of cosmic ray (%) received by Earth during November 18–22, 2003. Data downloaded from http://neutronm.bartol.udel.edu/~pyle/bri_table.html

4 Conclusion

The ICME event from November 18 to 22, 2003, is the largest geomagnetic storm of solar cycle 23 with a Dst index of – 472 nT. It immensely affected the ionosphere, magnetosphere, and cosmic rays received by the Earth, which is also seen during our study.

Moreover, the following points are the main conclusion that came from our study of the event:

1. When the CME of 18 November resulted in a solar storm of 20 November, the SYM-H decreased by approximately 500 nT, AE increased by around 4000 nT, and Bz was recorded at a minimum of around 55 nT. The solar wind pressure fluctuated between 2 Pa, 18 Pa, and density varied in the range of 30–5 kg/m^3 in the same pattern.
2. On the basis of our analysis of solar cycle 23 (1996–2008), we concluded that solar super storm can occur anytime in solar cycle. Its occurrence is independent of the phase of solar cycle and has possibility of occurrence anytime in solar maxima or in solar minima.
3. It is found that the total amount of energy in the form of ring current in our study is less than that of as studied by Gonzalez and Mac-Mohan in 1997.
4. The variation on TEC in all four stations was mainly due to the difference in latitude and the local time. However, one striking similarity of the wave nature in increment and decrement of TEC was observed in all the stations.
5. In all neutron monitor stations analyzed here, the rate of cosmic ray received decreases by approximately 3% during the ICME. From this analysis, it can be inferred that there exist inverse relation between the strength of solar storm and the amount of cosmic ray received by the Earth.

Thus, we can say that the study of the storm of this sort help us to better understand he conditions of different geomagnetic parameters during disturbed period. Moreover, we can also predict their affects in the space weather by analyzing the energetic particle precipitation, cosmic ray received by Earth during the storm period.

Acknowledgements The data for solar wind parameters and sunspot study was taken from https://omniweb.gsfc.nasa.gov/form/omni_min.html.The data for magnetic components, and galactic cosmic ray data was taken from http://www.intermagnet.org/ and http://neutronm.bartol.udel.edu/~pyle/bri_table.html respectively. The ionospheric total electron content data was downloaded from ftp://cddis.gsfc.nasa.gov/pub/gps/data.

Compliance with ethical standards

Conflict of interest The author(s) declare that they have no competing interests.

References

1. Adhikari B (2015) HILDCAA-related effects recorded in middle low latitude magnetometers. InstitutoNacional de PesquisasEspaciais, Sao Jose dos Campos
2. Adhikari B, Sapkota N, Baruwal P, Chapagain NP, Braga CR (2017) Impacts on cosmic-ray intensity observed during geomagnetic disturbances. Sol Phys 292(10):149
3. Adhikari B, Dahal S, Chapagain NP (2017) Study of field- aligned current (FAC), interplanetary electric field component (Ey), interplanetary magnetic field component (Bz), and northward (x) and eastward (y) components of geomagnetic field during supersubstorm. Earth Space Sci 4:257–274

4. Akasofu SI (1981) Energy coupling between the solar wind and the magnetosphere. Space Sci Rev 28:121–190
5. Arnold F (2006) Atmospheric aerosol and cloud condensation nuclei formation: a possible influence of cosmic rays? Space Sci Rev 125(1–4):169–186
6. Belov A, Abunin A, Abunina M, Eroshenko E, Oleneva V, Yanke V, Papaioannou A, Mavromichalaki H, Gopalswamy N, Yashiro S (2014) Coronal mass ejections and non-recurrent Forbush decreases. Sol Phys 289(10):3949–3960
7. Blanco JJ, Catalán E, Hidalgo MA, Medina J, García O, Rodríguez-Pacheco J (2013) Observable effects of interplanetary coronal mass ejections on ground level neutron monitor count rates. Sol Phys 284(1):167–178
8. Buonsanto MJ (1999) Ionospheric storm—a review. Space Sci Rev 88:563–601
9. Carslaw KS, Harrison RG, Kirkby J (2002) Cosmic rays, clouds, and climate. Science 298(5599):1732–1737
10. Chapman S, Ferraro VC (1930) A new theory of magnetic storms. Nature 126(3169):129
11. Chapman S, Ferraro VCA (1931) A new theory of magnetic storms. J Geophys Res 3(6):77–97
12. Chen J (1996) Theory of prominence eruption and propagation: interplanetary consequences. J Geophys Res 101:27499–27520
13. Daglis IA, Thorne RM, Baumjohann W, Orsini S (1999) The terrestrial ring current: origin, formation, and decay. Rev Geophys 37:407–438
14. Danilov AD, Lăstovička J (2001) Effects of geomagnetic storms on the ionosphere and atmosphere. Int J Geomagn Aeron 2:209–224
15. Dessler AJ, Parker EN (1959) Hydromagnetic theory of geomagnetic storms. J Geophys Res 64(12):2239–2252
16. Dubey SC, Mishra AP (1999) Solar activity and large geomagnetic disturbances. Curr Sci Assoc 77:293–296
17. Dumbović M, Devos A, Vršnak B, Sudar D, Rodriguez L, Ruždjak D, Leer K, Vennerstrøm S, Veronig A (2015) Geoeffectiveness of coronal mass ejections in the SOHO era. Sol Phys 290(2):579–612
18. Fagundes PR, Cardoso FA, Fejer BG, Venkatesh K, Ribeiro BAG, Pillat VG (2016) Positive and negative GPS- TEC ionospheric storm effects during the extreme space weather event of March 2015 over the Brazilian sector. J Geophys Res Space Phys 121:5613–5625. https://doi.org/10.1002/2015ja022214
19. Forbush SE (1937) On the effects in cosmic-ray intensity observed during the recent magnetic storm. Phys Rev 51(12):1108
20. Gonzalez WD, Gonzalez AC, Tsurutani BT (1990) Dual-peak solar cycle distribution of intense geomagnetic storms. Planet Space Sci 38(2):181–187
21. Gonzalez WD, Tsurutani BT, De Gonzalez ALC (1999) Interplanetary origin of geomagnetic storms. Space Sci Rev 88(3–4):529–562
22. Gopalswamy N, Tsurutani B, Yan Y (2015) Short-term variability of the sun-earth system: an overview of progress made during the CAWSES-II period. Prog Earth Planet Sci 2:13
23. Gopalswamy N, Yashiro S, Michalek G, Xie H, Lepping RP, Howard RA (2005) Solar source of the largest geomagnetic storm of cycle 23. Geophys Res Lett 32(12)
24. Guido RMD (2016) Coronal mass ejections during geomagnetic storms on earth. Int J Astron 5(2):19–24
25. Guido RMD (2018) Characterizing coronal mass ejections in solar cycle analysis. arXiv preprint arXiv:1804.10870
26. Hathaway DH (2007) The solar cycle. In: Guido RMD (2018) Characterizing coronal mass ejections in solar cycle analysis. arXiv preprint arXiv:1804.10870
27. Hess VF, Demmelmair A (1937) World-wide effect in cosmic ray intensity, as observed during a recent magnetic storm. Nature 140(3538):316
28. Immel TJ, Mannucci AJ (2013) Ionospheric redistribution during geomagnetic storms. J Geophys Res Space Phys 118:7928–7939. https://doi.org/10.1002/2013ja018919
29. Kudela K (2009) On energetic particles in space. ActaPhysicaSlovaca. Rev Tutor 59(5):537–652
30. Kumar A (2014) Interplanetary coronal mass ejections, associated features, and transient modulation of galactic cosmic rays. Sol Phys 289(6):2177–2205
31. Manchester WB, Gombosi TI, De Zeeuw DL, Sokolov V, Roussev I, Powell KG (2005) Coronal mass ejection shock and sheath structures relevant to particle acceleration. Astrophys J 622:1225–1239
32. Mendillo M, Klobuchar JA (2006) Total electron content: synthesis of past storm studies and needed future work. Radio Sci. 41:RS5S02. https://doi.org/10.1029/2005rs003394
33. Mendillo M (2006) Storms in the ionosphere: patterns and processes for total electron content. Rev Geophys 44:RG4001. https://doi.org/10.1029/2005RG000193
34. Nayak C, Tsai L-C, Su S-Y, Galkin IA, Tan ATK, Nofri E, Jamjareegulgarn P (2016) Peculiar features of the low-latitude and midlatitude ionospheric response to the St. Patrick's Day geomagnetic storm of 17 March 2015. J Geophys Res Space Phys 121:7941–7960. https://doi.org/10.1002/2016ja022489
35. Parker EN (1958) Interaction of the solar wind with the geomagnetic field. The Phys Fluids 1(3):171–187
36. Prölss GW (1995) Ionospheric F region storms. In: Volland H (ed) Handbook of atmospheric electrodynamics, vol 2. CRC Press, Boca Ration, pp 195–248
37. Prölss GW, Jung MJ (1978) Travelling atmospheric disturbances as a possible explanation for daytime positive storm effects of moderate duration at middle latitudes. J Atmos Solar Terr Phys 40:1351–1354. https://doi.org/10.1016/0021-9169(78)90088-0
38. Prölss GW (2008) Ionospheric storms at mid-latitude: a short review, in midlatitude ionospheric dynamics and disturbances. In: Kintner PM et al (eds) Geophys. Monogr. Ser, vol 181. AGU, Washington, D. C, pp 9–24. https://doi.org/10.1029/181gm03
39. Raizada A, Kumar S, Khare S (2010) Dependence of successive GMSs with Dst ≤ 100 nT on solar and interplanetary parameters. Indian J Phys 84(2):183–192
40. Rathore BS, Kaushik SC, Bhadoria RS, Parashar KK, Gupta DC (2012) Sunspots and geomagnetic storms during solar cycle-23. Indian J Phys 86(7):563–567
41. Mac-Mahon RM, Gonzalez WD (1997) Energetics during the main phase of geomagnetic superstorms. J Geophys Res 102(A7):14199–14207. https://doi.org/10.1029/97ja01151
42. Singh DK, Singh RP, Kamra AK (2004) The electrical environment of the Earth's atmosphere: a review. Space Sci Rev 113(3):375–408
43. Siingh D, Singh RP, Kamra AK, Gupta PN, Singh R, Gopalakrishnan V, Singh AK (2005) Review of electromagnetic coupling between the Earth's atmosphere and the space environment. J Atmos Solar Terr Phys 67(6):637–658
44. Siingh D, Gopalakrishnan V, Singh RP, Kamra AK, Singh S, Pant V, Singh R, Singh AK (2007) The atmospheric global electric circuit: an overview. Atmos Res 84(2):91–110
45. Siingh D, Singh RP (2010) The role of cosmic rays in the Earth's atmospheric processes. Pramana 74(1):153–168
46. Singh AK, Siingh D, Singh RP (2010) Space weather: physics, effects and predictability. Surv Geophys 31(6):581–638
47. Siingh D, Singh RP, Singh AK, Kulkarni MN, Gautam AS, Singh AK (2011) Solar activity, lightning and climate. Surv Geophys 32(6):659
48. Storini M (1990) Galactic cosmic-ray modulation and solar-terrestrial relationships. IlNuovoCimento C 13(1):103–124
49. Tinsley BA (2008) The global atmospheric electric circuit and its effects on cloud microphysics. Rep Prog Phys 71(6):066801

50. Tripathi SN, Michael M, Harrison RG (2008) Profiles of ion and aerosol interactions in planetary atmospheres. In: Planetary atmospheric electricity, Springer, New York, pp 193–211
51. Tsurutani BT, Gonzalez WD, Tang F, Lee (1992) Geophys Res Lett 19:73
52. Velinov PIY, Mishev A (2007) The induced ionization by solar cosmic rays in the earth atmosphere e CORSIKA code simulations. CR Acad Bulg Sci 60:493–500
53. Zhang J, Dere KP, Howard RA, Bothmer V (2003) Identification of solar sources of major geomagnetic storms between 1996 and 2000. Astrophys J 582:520–553